Reprinted from the Journal of Applied Mechanics,
Volume 41, Number 2, pages 484-490, June 1974

Numerical Solution of Non-Hertzian Elastic Contact Problems[1]

Krishna P. Singh
President and CEO
Holtec International
Marlton, NJ

and

Burton Paul

A general method for the numerical analysis of frictionless nonconformable non-Hertzian contact of bodies of arbitrary shape is developed. Numerical difficulties arise because the solution is extremely sensitive to the manner in which one discretizes the governing integral equation. The difficulties were overcome by utilizing new techniques, referred to as the method of redundant field points (RFP) and the method of functional regularization (FR). The accuracy and efficiency of the methods developed were tested thoroughly against known solutions of Hertzian problems. To illustrate the power of the methods, a heretofore unsolved non-Hertzian problem (corresponding to the case of rounded indentors with local flat spots) has been solved.

1 Introduction

The three-dimensional problem of contacting, nonformal,[2] elastic surfaces was solved by Hertz [8][3] for the restricted class of surfaces which are quadratic (i.e., second degree polynomials) near the contact point. However, the Hertz theory is inadequate to treat the wide variety of technologically important problems where the surfaces cannot be modeled as locally quadratic. Problems of this type arise in roller bearings with crowned (i.e., rounded) edges, in ball bearings with small corrosion pits, in loosely fitted pin joints, etc.

In this paper, we will establish numerical techniques for the solution of contact stress problems with frictionless surfaces that are nonconformal, but otherwise arbitrary. When the surfaces are not quadratic, we will call the problem "non-Hertzian."

An attempt to solve for the particular problem of fourth degree paraboloids in contact was made by Mow, Chow, and Ling [13] who admitted to only partial success. An earlier attempt by Cattaneo [1] for the special case of axisymmetric surfaces is briefly described by Lubkin [11].

More recently, Conry and Seireg [2], and Kalker and Randen [9], proposed numerical solutions to the contact problem using optimization techniques. These solutions appear to predict the compliance quite well, although the contact area and pressure distribution may not be determined accurately.

There is a wide literature (Luré [12]) dealing with flat-faced indentors (or stamps) wherein the contact area is known *a priori*. Although we specifically exclude such problems in this paper, we are indebted to a referee who pointed out the existence of the paper by Conway, et al. [3], which deals mainly with flat indentors, but does contain a brief discussion of the infinitely long circular cylinder indenting an elastic slab of finite thickness. This problem, which reduces to a Hertz problem for infinitely thick slabs, was solved by a method utilizing a stepwise constant pressure field, but differs in all other significant respects from the present paper.

In Section 2 of this work we reformulate the non-Hertzian contact problem, and introduce the concept of a family of "interpenetration curves" which serve as first (or final) approximations to the boundaries of the contact region Ω. This formulation leads to a singular integral equation of first type, which may be discretized in a manner described in Section 3. Since solutions to integral equations of the first type do not necessarily exist for any given kernel, small numerical errors can produce completely meaningless solutions, and attempts at a direct numerical ("simply discretized") solution are beset with difficulties. Such problems are reminiscent of the ill-posed problems, discussed by Hadamard [7], whose solutions do not depend continuously on the numerical data given. Fortunately, however, the problem is "properly posed" in the sense of Tychonov [19, 20]. This means that the problem makes sense physically, and a physically meaningful solution can be obtained despite the extreme sensitivity of the results to small deviations in the input data. Two methods, namely, the "Functional Regularization Method" (FR method) and "Redundant Field Point Method" (RFP method) are developed to overcome the numerical difficulties in the solution procedure.

---

[1] Part of a dissertation submitted by K. P. Singh as partial fulfillment of requirements for the Degree of PhD at the University of Pennsylvania.

[2] Curved surfaces are said to be nonconformal if all dimensions of the contact region Ω are small compared to the smallest radius of curvature of any normal section of the surfaces. Initially flat surfaces (stamps) will not be considered.

[3] Numbers in brackets designate References at end of paper.

Contributed by the Applied Mechanics Division and presented at the Winter Annual Meeting, Detroit, Mich., November 11-15, 1973, of The American Society of Mechanical Engineers.

Discussion on this paper should be addressed to the Editorial Department, ASME, United Engineering Center, 345 East 47th Street, New York, N. Y. 10017, and will be accepted until July 20, 1974. Discussion received after this date will be returned. Manuscript received by ASME Applied Mechanics Division, December, 1972. Paper No. 73-WA/APM-11.

The RFP method, described in Section 4, enables one to find the contact region, the pressure distribution and the *approach* with great accuracy. Numerical studies in Section 5 show that the RFP method also furnishes accurate determination of the pressure and the approach, but it may not predict the contact region with high precision. However, the RFP method provides a computationally fast and inexpensive means for obtaining the load versus approach relation.

The FR method, developed in Section 6, is shown to predict extremely accurate results even where the RFP method is ineffective.

Confidence in the numerical predictions of the RFP and FR methods is established by comparison with the known theoretical results for Hertzian problems. These methods are then applied, in Section 7, to a non-Hertzian problem, for which no theoretical solution is known.

2 Formulation of the Contact Problem

Let the two bodies be denoted as body 1 and body 2. Cartesian coordinate axes are set up for each body with the initial contact point as common origin. Axes (x_1, y_1) and (x_2, y_2) lie in the tangent plane of the two surfaces at the initial contact point, with z_1 and z_2 pointing into bodies 1 and 2, respectively. Both surfaces are frictionless and the external load is assumed to consist of a pair of compressive forces, F, along the axes of z_1 and z_2. Due to the applied force, material points in the two bodies undergo rigid-body translation and elastic deformation. For points on the surface of the body, it can be shown from geometric considerations (see, for example, Luré [12, p. 320]) that

$$w_1 + w_2 + z_1 + z_2 - \delta \geq 0 \tag{1}$$

where w_1 and w_2 are elastic displacements in the directions of z_1 and z_2, and δ is the relative approach, defined as the displacement of a point on one of the bodies, relative to a point on the second body, where both points are far removed from the contact region.

For those points which coalesce within the contact region, it is required that

$$w_1 + w_2 + z_1 + z_2 = \delta \tag{2}$$

Outside of the contact region, the condition of impenetrability requires that

$$w_1 + w_2 + z_1 + z_2 - \delta > 0 \tag{3}$$

For the class of problems under consideration, the dimensions of the contact region are assumed to be very small compared to local radii of curvature of the indenting surfaces. Hence it is permissible to consider the two bodies as elastic half spaces in order to correlate the displacement field w with the pressure field p inside the contact region Ω. For points on the frictionless surfaces of the bodies, w and p are related by integrating the Boussinesq solution for a normal point load, which leads to the following equation (Timoshenko, [17, p. 365]):

$$w_i(x, y) = \frac{(1 - \nu_i^2)}{\pi E_i} \int_\Omega \frac{p(x', y')dx'dy'}{[(x - x')^2 + (y - y')^2]^{1/2}}; \quad (i = 1, 2) \tag{4}$$

where ν_i and E_i are Poisson's ratios and Young's moduli of the two bodies, and Ω is the projection of the contact region on the tangent plane (xy). Because the two bodies cannot exert tension upon one another, a physically meaningful solution requires that

$$p(x, y) \geq 0 \text{ inside } \Omega \tag{5}$$

Conditions (2)–(5) define the contact problem which must be solved to obtain the pressure field p, contact region Ω and approach δ for a given normal force F. Equilibrium requires that

$$F = \int_\Omega p dA \tag{6}$$

The contacting surfaces may be described *a priori* by equations of the form: $z_1 = f_1(x, y)$; $z_2 = f_2(x, y)$. The relative initial separation defined by

$$f(x, y) = z_1 + z_2 = f_1(x, y) + f_2(x, y) \tag{7}$$

will be called the "profile function." Equations (2), (4), and (7) may be combined to yield

$$k \int \frac{pdA}{r} = k \int_\Omega \frac{p(x', y')dx'dy'}{[(x - x')^2 + (y - y')^2]^{1/2}} = \delta - f(x, y) \tag{8}$$

where the "elastic parameter" is defined by

$$k = (1 - \nu_1^2)/\pi E_1 + (1 - \nu_2^2)/\pi E_2$$

The half-space assumption originally employed by Hertz to correlate the displacement and pressure fields has been supported by various experimental investigations including some by Hertz himself. Experimental work by Fessler and Ollerton [5] indicates that this assumption is accurate for those Hertzian contact problems where the semimajor diameter of the contact ellipse is as large as half the smallest radius of curvature of either body. For non-Hertzian problems such bounds are not known to the best of our knowledge, but it is reasonable to assume that the assumption will be valid so long as the surfaces are nonconformal.

A principal difficulty in solving non-Hertzian contact problems is lack of *a priori* knowledge of the contact region, which is to be used as the domain of integration in equation (8).

In this work, we introduce a means of establishing a suitable family of closed curves which represent the contact boundaries for a given pair of body profiles. The pressure distribution, associated load, and approach are then computed. This procedure inverts the usual formulation of the problem where the load (or approach) is assumed given and the contact region is unknown.

To aid us in establishing the contact boundary for a given pair of indentors let us introduce the concept of the "interpenetration curve." The interpenetration curve is defined as the intersection of the two (undeformed) indentor surfaces if the vertex of the body 1 is moved along the axis z_2, through an arbitrary distance d. Note that such an interpenetration is strictly conceptual and violates the condition of impenetrability of solid materials. Different choices of the parameter d (henceforth called "interpenetration") give rise to the family of interpenetration curves described by the equation

$$f(x, y) = f_1(x, y) + f_2(x, y) = d \tag{9}$$

which represents the projection of the space curve of intersection onto the tangent plane at the contact point.

The family of interpenetration curves may be thought of as candidate contact boundaries associated with some family of applied loads. In the case of axisymmetric contact problems (e.g., arbitrary coaxial bodies of revolution, or two cylinders of equal diameters with their axes at right angles) the contact area is necessarily a circle and so are the interpenetration curves; i.e., circular interpenetration curves constitute a valid family of contact boundaries for a set of normal loads which remain to be determined.

When the interpenetration curves are not circles, they will not in general represent any member of the family of true contact boundaries. For example, in the general case of Hertzian contact (indentors are locally approximated by second degree surfaces), both the interpenetration curves and the contact boundaries are each represented by a family of similar ellipses; however, the aspect ratio of the two families differ, as shown in Singh [15].

For cases where the interpenetration curves do not match the true contact boundaries, they provide the basis (as will be shown) for an iterative procedure which rapidly converges to the true solution. Furthermore, it will be seen that, even if one does not refine the interpenetration curve by iteration, there results an ex-

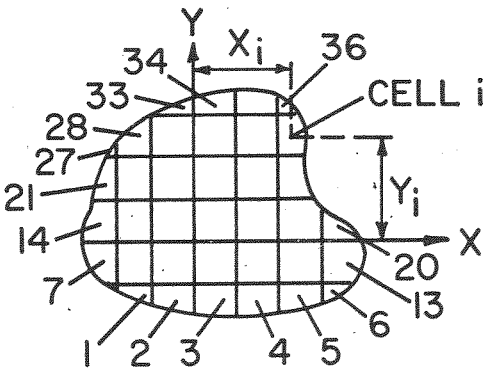

Fig. 1 Subdivided and labeled contact region

cellent approximation to the load versus approach curve, and to the peak contact pressure.

3 Simply Discretized Numerical Solution

For an arbitrary choice of parameter d, equation (9) provides a (possibly tentative)[4] candidate contact boundary surrounding the region Ω. For the "known" contact region Ω, equation (8) becomes a singular integral equation of the first kind in two dimensions with a singularity in the kernel at point $(x, y) = (x', y')$. We now consider that the approach δ, and contact pressure $p(x, y)$ are dependent variables, to be solved for the particular contact region Ω associated with the arbitrary choice of interpenetration d.

The operators in equation (8) must be discretized for a numerical solution. For this purpose, the contact region Ω is subdivided into n cells, each of which is given an integer label i (as in Fig. 1). For convenience, these cells may be rectangular[5] inside the boundary, and may be polygonal at the boundary which is approximated by straight line segments. The centroids (x_i, y_i) of the cells are considered "field points," and the pressure in each cell, is considered to be a constant p_i. The double integral in equation (8) is evaluated, for each field point, by iterated numerical quadrature, resulting in a linear algebraic equation in all of the p_i and the approach δ. Equation (8) is valid for each of the n field points. A singularity occurs in equation (8) at the field point i where $(x_i, y_i) = (x', y')$. The singularity is treated by isolating cell i and expressing the integral of $1/r$, over the polygonal cell i, in terms of elementary functions. Thus for the ith field point, equation (8) yields

$$kp_i \int_{A_i} (dA/r) + k \sum_{\substack{j=1 \\ j \neq i}}^{n} p_j \int_{A_i} (dA/r) = \delta - f_i, \qquad (10)$$

where A_i denotes the region of cell i, and f_i is the value of the profile function at (x_i, y_i). To a first approximation,

$$I_{ij} = \int_{A_i} dA/r \doteq A_j/r_{ij}, \qquad (j \neq i) \qquad (11)$$

where r_{ij} is the distance between field points i and j. It is shown in Singh [15] that a more accurate evaluation of the integral (equation (11)) entails considerably more computation and does not significantly improve the accuracy of the solution.

Since equation (10) is valid for every one of the n field points, n linear algebraic equations in $(n + 1)$ unknowns (n pressures p_i and the approach δ) are generated. These equations are of the form

[4] Until further notice we will assume that equation (9) describes a true contact boundary. Methods of refining Ω are described later.

[5] It is shown by Singh [15] that the minimum discretization error occurs when the rectangles are squares.

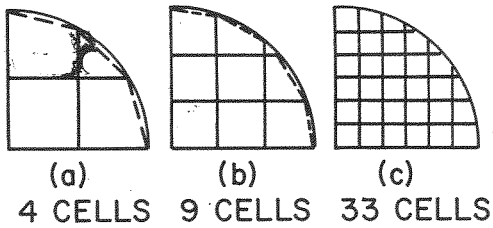

Fig. 2 Typical cell layouts for circular contact region

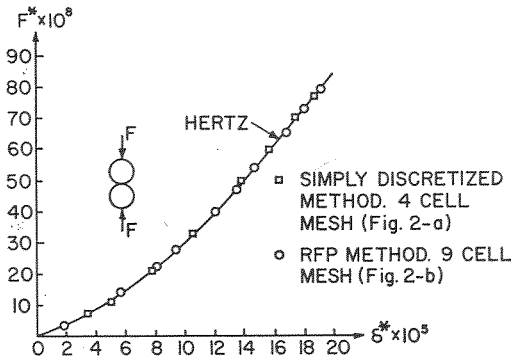

Fig. 3 Load versus approach for equal spheres

$$b_{ij}p_j = \delta - f_i, \qquad (i = 1, 2, \ldots, n) \qquad (12)$$

(where summation over the repeated index for the appropriate range is implied in equation (12) and all subsequent equations).

An additional independent equation is required to uniquely solve for the $(n + 1)$ unknowns of the problem.

To generate this equation, equation (8) is discretized at a convenient additional field point (for example, at the initial contact point), thereby providing the additional required equation:

$$V_j p_j = \delta - f_{n+1} \qquad (13)$$

Equation (13) may be used to eliminate δ from equations (12), thereby producing a system of the form

$$B_{ij}p_j = F_i, \qquad (i = 1, 2, \ldots, n) \qquad (14)$$

where $B_{ij} = b_{ij} - V_j$, and $F_i = f_{n+1} - f_i$. Equations (13) and (14) can be solved, in principle, to give what will be termed a "simply discretized" numerical solution. However, it will be found that such simple solutions are defective, because of the ill-posed nature of the problem, hence a direct solution of equations (14) will be found to yield nonsensical results. To illustrate this numerical sensitivity, consider the following problem.

Example 1. Two spheres of radii R_1 and R_2 are pressed together by a force F acting along the initial line of centers. It is recognized from symmetry that the contact area is circular. The profile function (defined by equation (7)) is given by

$$f(r) = f_1(r) + f_2(r) = R_1 - [R_1^2 - r^2]^{1/2} + R_2 - [R_2^2 - r^2]^{1/2} \qquad (15)$$

and the "quadratic approximation" to equation (15) is

$$f(r) = (r^2/2)(r_1^{-1} + r_2^{-1}) \qquad (16)$$

where r is distance of the field point from the center of the contact circle. Taking advantage of symmetry, we need only to subdivide one quadrant of the contact area into small cells. Figs. 2(a–c) show some possible mesh arrangements. For an assumed interpenetration d, the radius a of the contact circle is given by equations (9) and (16) in the form

$$d = \frac{a^2}{2}\left(\frac{1}{R_1} + \frac{1}{R_2}\right), \quad \text{or} \quad a = \left(\frac{2dR_1R_2}{R_1 + R_2}\right)^{1/2} \qquad (17)$$

Let $R_1 = R_2 = R$, and let n denote the number of cells per quadrant. For the case of $n = 4$, Fig. 2(a), the solution of equations (13) and (14) is found without any difficulty. The load versus approach prediction is shown by the squares in Fig. 3.

All subsequent numerical results will be expressed in terms of the following nondimensional quantities:

Approach: $\delta^* = \delta/R$; Semidiameters: $a^* = a/R$, $b^* = b/R$

Interpenetration: $d^* = d/R$; Pressure: $p^* = kp$

Radius: $r^* = r/R$; Force: $F^* = kF/R^2$

Coordinates: $x^* = x/R$, $y^* = y/R$,

where, in general

$$R^{-1} = (1/4)(r_{11}^{-1} + r_{12}^{-1} + r_{21}^{-1} + r_{22}^{-1}) \tag{18}$$

In equation (18) r_{11}, r_{12} are the principal radii of curvature for body 1, and r_{21}, r_{22} are those for body 2.[6]

Note that the predicted relationship between load and approach is in excellent agreement with Hertz's analytical solution shown by the solid curve. Although the load versus approach relation is predicted excellently, the individual values of load and approach for any assumed contact radius are not predicted quite as accurately, being in error by 10 percent, typically.

From the foregoing results we are encouraged to try a somewhat finer mesh division. However, at the next higher cell density, $n = 9$, Fig. 2(b), the ill-posed naure of the problem invalidates the simple solution. The pressures at some field points turn out to be negative which is not acceptable.

When first confronted with the numerical difficulties of the simply discretized method, we suspected that the system of equations was ill-conditioned. Upon investigating all the common sources of ill-conditioning [15] it was concluded that the difficulties cannot be cured by the usual treatments (e.g., scaling techniques, or carrying sufficient digits to control roundoff error). In fact, the difficulties are due to the inherently ill-posed nature of the problem and require unusual remedies. We have devised two methods to overcome the numerical difficulties; the first of these, the "Method of Redundant Field Points" (RFP) is described next, and the second, the method of "Functional Regularization" (FR) is described in Section 6.

4 Method of Redundant Field Points (RFP)

Since extremely accurate solutions of the simply discretized equations (13) and (14) produce physically meaningless results, we are led to believe that the fault lies in the discretized equations themselves. Apparently, the method of discretization used has introduced significant errors in the coefficients of the algebraic equations. An attempt to reduce the errors by using more accurate quadrature formulas than those described in Section 3 did not produce a significant improvement in the results. Therefore we looked elsewhere for the source of errors, and reasoned as follows.

Each linear equation of type (12) has errors in the coefficients b_{ij}. If we exactly solve n such equations for n unknowns, we get the solution to some problem other than the desired one. If, however, we formulate more than n equations of type (12) there is a possibility that the errors in b_{ij} will be of a random nature. Hence a suitable "averaging" of the redundant coefficients b_{ij} may result in a cancellation of the random errors. Such an "averaging technique," of course, is the well-known method of least squares used for curve fitting of experimental data. Therefore, we are motivated to generate m redundant linear equations

[6] The definition (18) is introduced for later convenience; in this example $R = R_1 = R_2$.

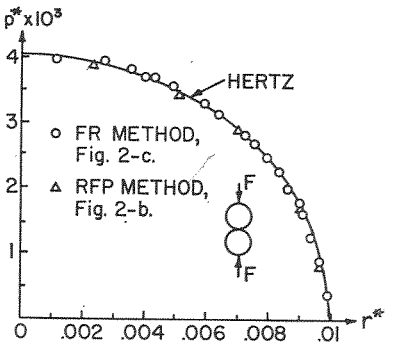

Fig. 4 Pressure distribution identical spheres in contact; $F^* = 0.849 \times 10^{-6}$

(in the n unknowns p_i) corresponding to a discretized version of the integral equation (8) for m additional field points (x, y). Having found $(m + n)$ approximate equations in the n unknowns p_i, we take an "experimental" point of view and seek that solution set p_i, which "best satisfies" (i.e., in the sense of least-square error criterion) the $(m + n)$ approximate equations.

One convenient way to generate the m redundant equations is to utilize the nodes of the cells (previously we used the centroids of the cells) as field points in equations (8). Accordingly, equation (14) takes the form

$$B_{ij}p_j = F_i; \qquad i = 1, 2, 3, \ldots, (n + m) \tag{19}$$

The mean-square error ϵ^2 is thus seen to be given by

$$(n + m)\epsilon^2 = (B_{ij}p_j - F_i)(B_{ik}p_k - F_i) \tag{20}$$

For a minimum of ϵ^2 it is required that

$$(n + m)(\partial\epsilon^2/\partial p_l) = 2B_{ij}B_{il}p_j - 2B_{il}F_i = 0 \qquad l = 1, 2, \ldots, n \tag{21}$$

The solution of equation (21) amounts to solving the matrix system

$$[D]\{p\} = [B]^T[B]\{p\} = [B]^T\{F\} \tag{22}$$

Equation (22) is readily solved using Gaussian elimination.

Various Hertzian contact problems were solved by the method just described. These problems with known solutions served as test cases for the RFP method. The load versus approach curves for the many cases investigated showed excellent agreement with the analytical answers, even for coarse meshes.

Example 1 was solved using this method. Fig. 3 shows the predicted load versus approach relation for the mesh arrangement shown in Fig. 2(b) (recall that the simply discretized solution broke down for this meshwork). It is seen that the agreement with the Hertz solution is excellent. Fig. 4 shows the pressure as a function of distance from the origin, together with the Hertzian solution. Note the excellent agreement, despite the use of a coarse mesh. This method is extremely fast as well as accurate. For example, obtaining the pressure field, approach, and resultant load for any given contact radius takes less than 5 sec of computation time[7] for solving Example 1 using the mesh arrangements of Figs. 2(a, b).

The accuracy of the load-approach relation and the computational efficiency of the RFP method makes this method extremely attractive for the determination of the load versus approach relation for non-Hertzian problems. Furthermore, this method has been found to produce quick convergence to the true contact area for a wide range of Hertzian problems. This is discussed in detail in the next section.

As in all numerical methods, we expect the solution accuracy to

[7] Execution time for IBM 360/75 at $0.20 per sec.

improve with decreasing cell size until roundoff errors[8] dominate the process and cause a deterioration in accuracy for cells which are smaller than some optimum length. Because of the physically ill-posed nature of our problem, this deterioration can occur for a relatively coarse cell size, and we need some internal measure of solution accuracy.

Accordingly, the von Neumann-Goldstine [14] "condition criterion" is used to test the matrices $[D]$ appearing in equation (22) for any given cell size. This criterion states that the "condition" of a matrix $[D]$ is related to the product of the Euclidean norms $||D||$ and $||D^{-1}||$. Since our matrix $[D]$ is symmetric, it may be shown [6, p. 142], that

$$||D||\,||D^{-1}|| = \mu_{\max}/\mu_{\min} = L \tag{23}$$

where $\mu_{\min}$ and $\mu_{\max}$ are the largest and smallest eigenvalues of $[D]$. The smaller the value of the condition number L, the better the condition of the matrix $[D]$.

Numerous tests [15] have shown that solution accuracy of the RFP method improves with decreasing cell size until the minimum condition number L is reached, thereby defining the optimum cell size for a given problem.

In the case of Example 1, the optimum cell size was found to correspond to Fig. 2(*b*). The "solution" for a denser cell layout such as Fig. 2(*c*) is found to have greater error than the "optimal solution," when compared with the analytical solution.

5 Application of the RFP Method to Problems With Noncircular Contact Regions

It is shown in Singh [15] that the interpenetration curves will not necessarily coincide with noncircular contact boundaries. However, the interpenetration curve encloses a region Ω^* which may be used as an initial estimate of the contact region.

In some instances, it may be desirable to determine Ω with greater accuracy. This can be accomplished by using an iterative scheme. At any point (x_i, y_i) which is outside of, but near the contact region, condition (3) and equations (4) and (7) require that

$$e' \equiv k \int_{\Omega} \frac{p(x', y')dx'dy'}{[(x_i - x')^2 + (y_i - y')^2]^{1/2}} - \delta + f(x_i, y_i) > 0 \tag{24}$$

Note that field points (x_i, y_i) which lie outside of the contact boundary do not produce a singularity in the integrand of equation (24). Therefore, the integral shown in equation (24) can be readily calculated by means of equation (11). Having obtained $\{p\}$ based on Ω^*, equation (24) is used to examine the sign of e' for selected points in the immediate vicinity of the contact boundary. If some e' turns out to be negative, then it is necessary to examine more points further out from the assumed boundary. The locus of points where e becomes positive defines a new tentative region Ω_1. The boundary of the new contact area, Ω_2, is taken as the mean boundary between Ω_1 and Ω^*. Based on this new contact area, new $\{p\}$ and $\{\delta\}$ are found, and the iteration is continued until condition (24) is satisfied at all points in the immediate neighborhood of the contact area Ω_i.

In numerous trials, this scheme showed very rapid convergence, and normally no more than 2 or 3 iterations were required. The following two Hertzian contact problems illustrate the method:

Example 2. Circular cylinders with radii R_1, and $R_2 = 10R_1$, have their axes at right angles, Fig. 5. The cylinders have equal elastic properties. Using Hertz's solution (Love, [10]), we find that the aspect ratios of the interpenetration and contact ellipses are quite different; namely, 3.16 and 4.53, respectively. All nodes in the first quadrant except those at the boundary were used to provide the redundant field points.

The computed load versus approach relation based on Ω^* shows reasonable agreement with Hertz's solution, Fig. 5. This illustrates that the interpenetration curve can be an excellent basis for determining the load versus approach relation, even in extreme situations where Ω^* differs significantly from the true contact region.

[8] All numerical work was done with IBM 360 double precision arithmetic, i.e., approximately 16 significant decimal digits.

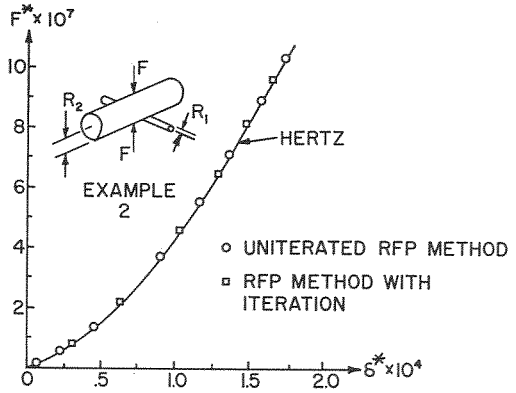

Fig. 5 Load versus approach, two crossed cylinders of radii R_1 and R_2, $R_2 = 10\,R_1$

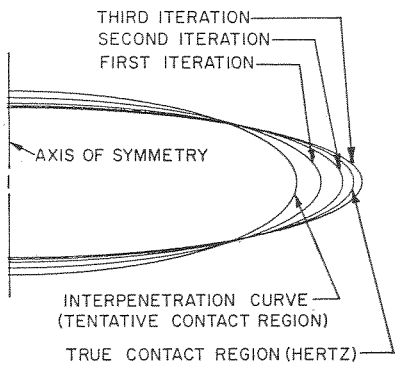

Fig. 6 Iteration on contact region; Example 2

Table 1 Comparison of RFP method with Hertz's analytical solution

Quantity	RFP method	Hertz	Percent error
δ^*	0.7961×10^{-4}	0.7961×10^{-4}	0 (assumed)
F^*	0.3101×10^{-6}	0.3178×10^{-6}	2.42
a^*	0.0171	0.0170[a]	0.589
b^*	0.00388	0.00380[a]	2.17[a]

[a] Estimated from graphs in Cooper [4].

The iteration scheme just described converged in 3 iterations to a contact ellipse which is extremely close to the Hertzian solution, Fig. 6. Fig. 5 also shows the load-approach curve corresponding to the iterated contact boundary. Table 1 shows how the RFP method compares with Hertz's analytical solution for one typical approach value.

Solutions of comparable accuracy were obtained for increasingly slender contact ellipses. Accuracy was found to fall off significantly for contact ellipses with aspect ratios in excess of 10.

Numerical studies, for decreasing aspect ratios of Ω, show that the predicted load versus approach relationship is always excellent. However, the iterations will not converge to the true contact region if the latter is nearly circular. Note, however, that if the contact region is known to be exactly circular, as in Example 1, the RFP method is adequate in all respects.

Therefore we see that the RFP method is extremely efficient and accurate when restricted to a well-defined range of applications. Outside of this range it is necessary to utilize another technique. Such a technique, the FR method, will now be described.

6 Functional Regularization Method

Outside of the range where the RFP method is applicable it is found that an infinite number of apparent solutions exist, in the sense that they satisfy equations (13) and (14) within extremely small residuals. Of these apparent solutions, only those which satisfy inequalities (3) and (5) are acceptable. In addition, we note that the class of problems under consideration requires that the variation in p along any straight line within any simply connected contact region must not oscillate violently.[9] This observation enables us to utilize the notion of a quasi-solution and the functional regularization scheme developed by Tychonov [18–20]. The particular variant of the FR method employed here has not yet been treated in the literature to the best of our knowledge. Assume that the cells in Fig. 1 are numbered sequentially from left to right, and from the bottom up for any given simply connected contact region. Let the cell number of the rightmost cell in row i be given by m_i. If there are q rows and a total of n cells, then $m_q = n$. Consider the auxiliary function Φ given by

$$\Phi = \sum_{j=1}^{q} \sum_{i=m_{(j-1)}+1}^{m_j-1} (p_i - p_{i+1})^2 \tag{25}$$

where $m_0 = 0$.

Φ is nonnegative and is zero (minimum) when all components of p in each row are equal. It is readily recognized that, out of a set of candidate $\{p\}$ vectors which approximately satisfy equations (13) and (14), that which has the smoothest variation (i.e., least mean-square point-to-point deviation) along each row of cells will make Φ a minimum. If desired, we could find the exact solution of equation (14). Unfortunately, the elements of $[B]$ are inexact, and therefore the exact solution vector $\{p\}_e$ is not the one we seek. Some elements of $\{p\}_e$ may be negative, and neighboring elements of $\{p\}_e$ may vary excessively. We seek to satisfy equation (14) in an average sense while keeping the point-to-point deviation in elements of $\{p\}$ reasonably small. In other words we seek a vector $\{p\}$ which does not satisfy equation (14) exactly but keeps $\epsilon^2 = \sum_i [B_{ij}p_j - F_i]^2$ small, and simultaneously keeps the auxiliary function Φ small. This will have the effect of "fairing" the p surface, and prohibiting large oscillations in p. Hence we seek a minimum of

$$\psi(p_i) = (B_{ik}p_k - F_i)(B_{ij}p_j - F_i) + \lambda\Phi \tag{26}$$

where λ is a suitably chosen small parameter. This implies solving the equation set

$$2B_{ij}B_{il}p_j + \lambda(\partial\Phi/\partial p_l) = 2B_{il}F_i \qquad l = 1, 2, \ldots, n \tag{27}$$

The following guidelines for a suitable choice of λ were established in (Singh [15], Singh and Paul [16]).

Let the relative error ϵ_f be defined by

$$\epsilon_f = \|[D]\{p\} - [B]^T\{f\}\| / \|[B]^T\{f\}\| \tag{28}$$

We can keep ϵ_f smaller than some tolerance TOL if λ is chosen such that

$$\lambda \geq \mu_{\min}\text{TOL}/4 \tag{29}$$

[9] Recall that the principal radii of curvature for the indenting surfaces must be large compared to the largest characteristic dimension of the contact region; this prohibits singularities in the pressure distribution, or excessively steep pressure gradients.

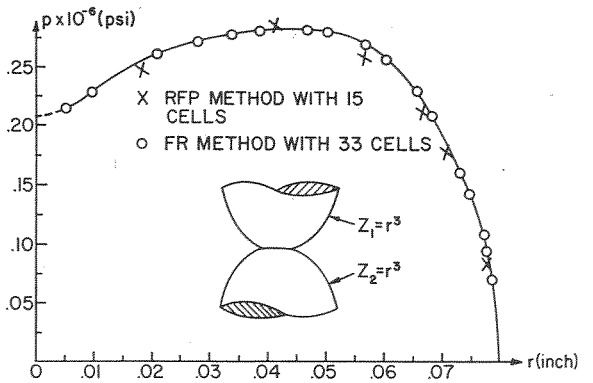

Fig. 7 Pressure distribution; cubic surfaces in contact, F = 4684 lb

where $\mu_{\min}$ is the numerically smallest eigenvalue of the symmetric matrix $[D]$, and is readily found by standard techniques such as Rayleigh's method. In practice we have had no difficulty in choosing TOL in range of 10^{-4} to 10^{-2}.

The numerical procedure is to choose the smallest value of λ consistent with condition (29), and to solve equation (27) for $\{p\}$.

The FR method was successfully applied to the examples discussed in Sections 4 and 6. Table 2 summarizes the numerical solution using the FR method for Example 1 with the mesh arrangement of Fig. 2(c), and the value $\lambda = 0.0133$. It should be recalled that the RFP method would not work with so fine a meshwork.

Fig. 4 shows a typical pressure distribution. It is seen that the agreement with the analytical solution is excellent.

In order to further test the FR method, we solved a number of Hertzian contact problems with contact ellipse aspect ratios: $1 \leq a/b \leq 10$. In all cases, complete convergence to the true contact region was achieved (within a tolerance specified as 0.05 of the semiminor diameter of the contact ellipse). It was stated in Section 5 that the redundant field point method could not produce good convergence to the contact boundary for aspect ratios close to 1, even though the load versus approach relation is in excellent agreement with the analytical solution. On the other hand, the functional regularization method handled all aspect ratios with equal ease, and the convergence to the contact boundary was always found to be fast (normally 3 or 4 iterations were required). Some numerical results for test cases may be found in Singh [15].

7 A non-Hertzian Contact Problem

To illustrate the generality of the method developed in this work, a non-Hertzian problem is solved in this section.

Example 3. Consider two surfaces given by

$$z_1 = \Lambda_1 r^3; \qquad z_2 = \Lambda_2 r^3 \tag{30}$$

where $r = (x^2 + y^2)^{1/2}$. The interesting feature of this problem is that the contact profiles are extremely "flat" (i.e., the radius of profile curvature is infinite at the contact point), as shown in Fig. 7. The surfaces are loaded by a force F along the axis of symmetry.

It is readily recognized that the profile function $f(x, y) = z_1 +$

Table 2 Comparison of FR method with Hertzian solution, numerical results for Example 1 (Fig. 2(c), 33 cells)

$d^* \times 10^2$ Interpenetration	$a^* \times 10^3$ (Contact radius)	$\delta^* \times 10^5$ Pred by FR method	$\delta^* \times 10^5$ Soln by Hertz	$F^* \times 10^9$ Pred by FR method	$F^* \times 10^9$ Soln by Hertz
0.01	1.000	0.1982	0.2	0.8464	0.8488
0.4	6.325	7.927	8.0	214.1	214.8
0.8	8.944	15.85	16.0	605.5	607.3
1.0	10.0	19.82	20.0	846.2	848.8

z_2 cannot even be approximated by quadratic terms in the x and y-coordinates. Hence the Hertzian theory is not adequate to solve this problem.

From symmetry, it is apparent that the contact region is circular. For an interpenetration d; the radius of the interpenetration circle a, follows from equations (9) and (30)

$$a = [d/(\Lambda_1 + \Lambda_2)^{1/3}] \tag{31}$$

The coefficient matrix $[B]$ and profile function vector $\{F\}$ of equation (14) are generated in a computer program in the same way as for a Hertzian problem. Both the RFP method and the FR method were used to solve this problem for $E_1 = E_2 = 30 \times 10^6$ psi, $\nu_1 = \nu_2 = 0.3$, and $\Lambda_1 = \Lambda_2 = 1$ in.$^{-2}$. Fig. 7 shows the pressure distribution and Fig. 8 shows the load and the contact radius versus the approach. The solutions predicted by both the RFP and the FR methods are in close agreement.

The "dip" in the pressure distribution, near the axis of symmetry, can be explained by the fact that the virtually flat central region is surrounded by a region of a relatively high curvature which serves as an effective "edge" on a flat punch. We would expect to see the contact pressure peak in the neighborhood of such edges.

Solutions for other non-Hertzian contact problems will be found in Singh [15].

8 Conclusions

A general three-dimensional theory of frictionless nonconformable non-Hertzian elastic contact has been developed which may be effectively used to analyze the stress concentrations and deflection patterns for almost arbitrary contacting profiles (which may include cavities, curvature discontinuities, etc.).

Because the governing integral equation of the first type is physically ill-posed, but is well-posed in the sense of Tychonov, we found it necessary to develop two new solution techniques.

The Redundant Field Point (RFP) method is efficient, and has built-in checks to define its range of applicability.

The Functional Regularization (FR) method has a wider range of applicability, and will suffice for most practical calculation needs.

Both methods were tested against known theoretical solutions for Hertzian contact problems, and were found to be extremely accurate in their respective ranges of applicability.

As an example of the power of these new numerical methods, a heretofore unsolved non-Hertzian contact problem was solved. Additional non-Hertzian problems have been solved by the methods of this paper, and are described in Singh [15].

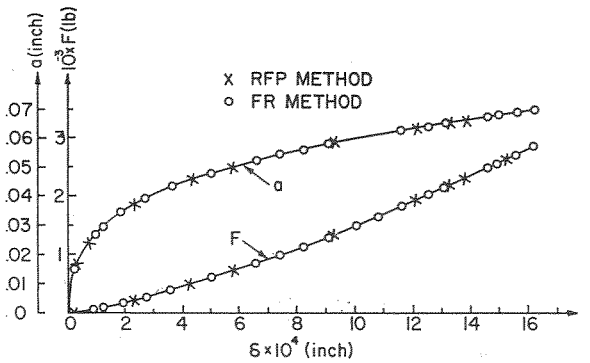

Fig. 8 Load (F) and radius (a) of contact region versus approach; cubics in contact

References

1 Cattaneo, C., "Teoria del contacto elastico in seconda approxximazione," University of Rome, *Rend. mat. appl.*, No. 6, 1947, pp. 504–512.

2 Conry, T. F., and Seireg, A., "A Mathematical Programming Method for Design of Elastic Bodies in Contact," JOURNAL OF APPLIED MECHANICS, Vol. 38, No. 1, TRANS. ASME, Vol. 93, Series E, Mar. 1971, pp. 388–392.

3 Conway, H. D., et al., "Normal and Shearing Contact Stresses in Indented Strips and Slabs," *International Journal of Engineering Science*, Vol. 4, 1966, pp. 343–359.

4 Cooper, D. H., "Table of Hertzian Contact Coefficients," Coordinated Science Laboratory, University of Illinois, Report No. R-387, 1968.

5 Fessler, H., and Ollerton, E., "Contact Stresses in Toroids Under Radial Loads," *British Journal of Applied Physics*, 8: 10, 1957, pp. 387–393.

6 Fox, L., *An Introduction to Numerical Linear Algebra*, Oxford University Press, New York, 1965.

7 Hadamard, J. H., *Lectures on Cauchy's Problem*, Dover Publications, New York, 1952, pp. 33–35.

8 Hertz, H., Miscellaneous papers (translated by Jones, D. E., and Schott, G. A.), Macmillan and Co.; London, 1896 Translation from: (*i*) "On the Contact of Elastic Solids," *Journal for die reine und angewandte mathematik*, Vol. 92, 1881, pp. 156–171; also (*ii*) "On the Contact of Rigid Elastic Solids and on Hardness," *Verhandlungen des Vereins zur Beforderung des Gewerbefleisses*, Nov. 1882.

9 Kalker, J. J., and Van Randen, Y., "A Minimum Principle for Frictionless Elastic Contact With Application to non-Hertzian Half Space Contact Problems," Private communication; to be published.

10 Love, A. E. H., *Mathematical Theory of Elasticity*, Dover, N. Y., 1927.

11 Lubkin, J. L., "Contact Problems," *Handbook of Engineering Mechanics*, ed., Flügge, W., McGraw-Hill, New York, 1962.

12 Luré, A. I., *Three-Dimensional Problems of the Theory of Elasticity*, Interscience, 1964.

13 Mow, V. C., Chow, P. L., and Ling, F. F., "Microslips Between Contacting Paraboloids," JOURNAL OF APPLIED MECHANICS, Vol. 34, No. 2, TRANS. ASME, Vol. 89, Series E, June 1967, pp. 321–378.

14 von Neumann, J. and Goldstine, H. H., "Numerical Inverting of Matrices of High Order," *Bulletin of the American Mathematical Society*, Vol. 53, 1947, pp. 1021–1099.

15 Singh, K. P., "Contact Stresses in Elastic Bodies With Arbitrary Profiles," PhD dissertation, University of Pennsylvania, 1972.

16 Singh, K. P., and Paul, B., "A Method for Solving Ill-Posed Integral Equations of the First Kind," *Computer Methods in Applied Mechanics and Engineering*, Vol. 2, 1973, pp. 339–348.

17 Timoshenko, S. P., and Goodier, J. N., *Theory of Elasticity*, 2nd ed., McGraw-Hill, New York, 1951.

18 Tychonov, A. N., "Regularization of Incorrectly Posed Problems," *Soviet Math*, Vol. 4, 1963, pp. 1624–1627.

19 Tychonov, A. N., "Solution of Incorrectly Posed Problems and the Regularization Method," *Soviet Math*, Vol. 4, 1963, pp. 1035–1038.

20 Tychonov, A. N., "Incorrect Problems of Linear Algebra and a Stable Method for Their Solution," *Soviet Math*, Vol. 6, 1965, pp. 988–991.